

Programmable Zwitterionic Droplets as Biomolecular Sorters and Model of Membraneless Organelles

Umberto Capasso Palmiero,* Carolina Paganini, Marie R. G. Kopp, Miriam Linsenmeier, Andreas M. Küffner, and Paolo Arosio*

Increasing evidence indicates that cells can regulate biochemical functions in time and space by generating membraneless compartments with well-defined mesoscopic properties. One important mechanism underlying this control is simple coacervation driven by associative disordered proteins that encode multivalent interactions. Inspired by these observations, programmable droplets based on simple coacervation of responsive synthetic polymers that mimic the “stickers-and-spacers” architecture of biological disordered proteins are developed. Zwitterionic polymers that undergo an enthalpy-driven liquid–liquid phase separation process and form liquid droplets that remarkably exclude most molecules are developed. Starting from this reference material, different functional groups in the zwitterionic polymer are progressively added to encode an increasing number of different intermolecular interactions. This strategy allowed the multiple emerging properties of the droplets to be controlled independently, such as stimulus-responsiveness, polarity, selective uptake of client molecules, fusion times, and miscibility. By exploiting this high programmability, a model of cellular compartmentalization is reproduced and droplets capable of confining different molecules in space without physical barriers are generated. Moreover, these biomolecular sorters are demonstrated to be able to localize, separate, and enable the detection of target molecules even within complex mixtures, opening attractive applications in bioseparation, and diagnostics.

organelles formed by liquid–liquid phase separation of nucleic acids and proteins.^[2–5] One of the most remarkable features of these biological condensates is their ability to create distinct compartments with different compositions without physical barriers.^[6,7] These membraneless compartments are important in the regulation of many biological processes.^[5,8]

Most of these biomolecular condensates are formed by macromolecules capable of encoding multivalent interactions and spontaneously promoting demixing. An important class of proteins associated with biomolecular condensates is represented by intrinsically disordered domains enriched in specific amino acids. These sequences, also referred to as low-complexity domains (LCDs),^[9–11] encode multiple attractive intermolecular forces including π – π , cation– π , hydrophobic, and charge–charge interactions.^[12,13] These interactions can be modulated by a variety of physical and chemical stimuli, allowing the organelles to dynamically adapt to the environment and to reversibly assemble and disassemble upon stress and nutrient starvation.^[3,4,14]

Phase separation is very well known in the field of synthetic polymers, which share several properties of LCDs including structural disorder and the ability to encode multivalent interactions responding to external cues, such as changes in temperature, salt concentration, and pH value. Associative and stimulus-responsive polymers have been broadly studied for almost a century^[15,16] and exploited in a variety of applications in bioprocessing and biomedicine. A few relevant examples, among many others, are poly(*N*-isopropylacrylamide) (PNIPAM), peptide polymers, and simple and complex coacervates.^[17–24]

In addition to stimulus-responsiveness, recent biological studies have shown that different protein LCDs are capable of modulating emerging properties of the compartments, such as viscosity, polarity, and the partitioning of different client molecules.^[25–27] These results demonstrate that the architecture of the scaffold component can control not only the stimulus-responsiveness but also several mesoscopic properties of the resulting compartments, which in turn are crucial for modulating the biochemical processes within them.^[25,27–33] However, the control of these mesoscopic properties with model polymers remains challenging. Complex coacervates have been shown to incorporate biomolecules, and researchers are starting to

1. Introduction

The temporal and spatial control of chemical processes in cells is a hallmark of life.^[1] In addition to membrane-bound compartments, an increasing body of evidence shows that spatial segregation of reactions can also be achieved via membraneless

U. Capasso Palmiero, C. Paganini, M. R. G. Kopp, M. Linsenmeier, A. M. Küffner, P. Arosio

Department of Chemistry and Applied Biosciences

Institute for Chemical and Bioengineering

ETH Zurich

Zurich 8093, Switzerland

E-mail: umberto.capasso@chem.ethz.ch; paolo.arosio@chem.ethz.ch

 The ORCID identification number(s) for the author(s) of this article can be found under <https://doi.org/10.1002/adma.202104837>.

© 2021 The Authors. Advanced Materials published by Wiley-VCH GmbH. This is an open access article under the terms of the Creative Commons Attribution-NonCommercial License, which permits use, distribution and reproduction in any medium, provided the original work is properly cited and is not used for commercial purposes.

DOI: 10.1002/adma.202104837

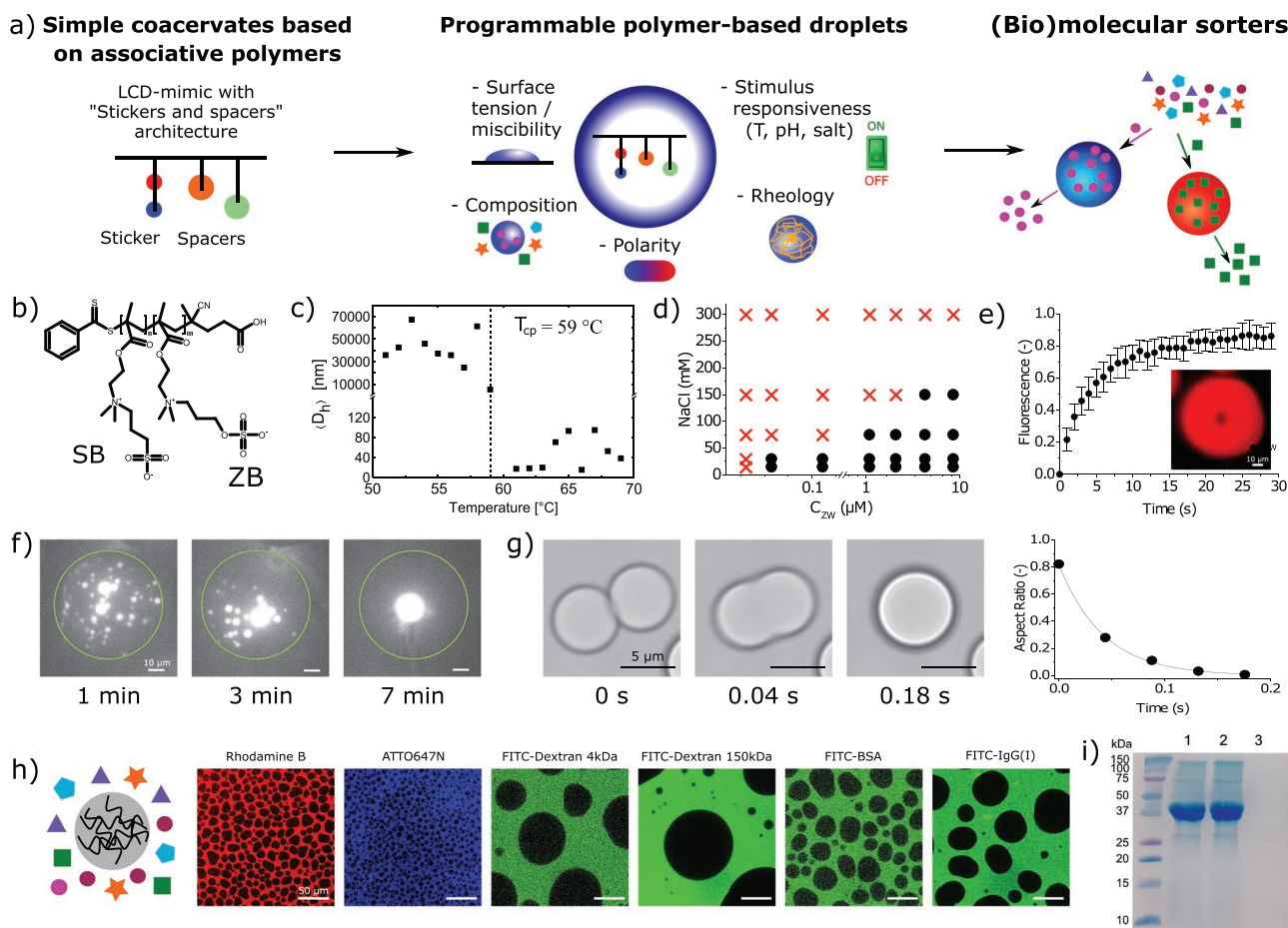


Figure 1. Zwitterionic polymers form responsive liquid droplets that largely exclude molecules. a) Design of associative polymers that undergo simple coacervation to generate programmable droplets with multiple desired properties. These droplets are a model of cellular compartments and can act as biomolecular sorters. b) Structure of the zwitterionic copolymers (ZW1, ZW2, and ZW3) containing ZB as sticker and SB as spacer in different ratios (Table S1, Supporting Information). c) Average hydrodynamic diameter of 0.5 mg mL^{-1} ZW2 aqueous solution at $30 \times 10^{-3} \text{ M}$ NaCl and $\text{pH} = 7.5$ as a function of temperature. d) Phase diagram of ZW2 at different polymer concentrations and ionic strengths. Red crosses and black circles indicate absence and presence of phase separation, respectively. e) Fluorescence recovery after photobleaching (FRAP) of ZW2 droplets. f) Merging of ZW2 droplets in microfluidic water-in-oil compartments and g) a fusion event in the bulk. h) Confocal microscopy images showing the preferential exclusion of several molecules from ZW2 droplets. Conditions: 0.25 mg mL^{-1} of ZW2 in $90 \times 10^{-3} \text{ M}$ NaCl together with $1 \times 10^{-6} \text{ M}$ of various molecules. The partition coefficients are: 0.414 ± 0.04 (rhodamine B), 0.54 ± 0.01 (ATTO647N), 0.08 ± 0.02 (dextran 4 kDa), 0.33 ± 0.08 (dextran 150 kDa), 0.13 ± 0.01 (BSA labeled with fluorescein isothiocyanate (FITC)), and 0.19 ± 0.01 (IgG(I)). i) SDS-gel analysis of molecules recruited into ZW2 droplets incubated in the presence of a cell lysate: 1) cell lysate, 2) supernatant after removal of ZW2 droplets, and 3) dissolved ZW2 droplets.

uncover rules underlying their uptake and release.^[34–36] Indeed, complex coacervates can mimic several features of biological condensates.^[37] Nevertheless, most of these polymeric coacervates are based on a single type of interaction (e.g., electrostatic), which can limit the programmability of the mesoscopic properties of the resulting compartments. In contrast, biological LCDs encode multiple interactions,^[12] which are likely required to simultaneously control multiple properties such as stimulus-responsiveness and incorporation of client molecules.^[25,38,39] A higher level of complexity in the model polymeric systems would, therefore, better mimic the biological behavior.

Here, inspired by the architecture of biological LCDs, we designed programmable liquid compartments based on the simple coacervation of associative polymers. These polymers incorporated multiple functional groups encoding different types of intermolecular interactions, which allowed us to

simultaneously control multiple mesoscopic properties of the droplets (Figure 1a).

2. Results and Discussion

First, we identified a reference polymeric material forming liquid droplets from which most molecules are largely excluded. The design of this polymer was inspired by the emerging “stickers and spacers” architecture of biological LCDs.^[13,40,41] Zwitterionic (ZW) copolymers containing different monomers were generated: one monomer functions as “sticker” and promotes the attractive interactions responsible for phase separation, and other monomers act as “spacers” and are intercalated between stickers. The monomer sulfobetaine methacrylate (ZB) was selected as the “sticker” due to its ability to induce phase

separation by ion-ion interactions.^[42,43] We initially considered the monomer sulfobetaine methacrylate (SB) as the “spacer” due to its good solubility in aqueous solutions (Figure 1b). Both zwitterionic monomers are known for their superhydrophilic properties and lack of protein adsorption.^[44,45] Thus, they could limit the recruitment of molecules within the droplets, thereby acting as an ideal reference material for the design of specific uptake of client molecules by further modulation of the polymer composition. We generated three copolymers with different ratios of stickers and spacers (ZW1, ZW2, and ZW3; their full characterization results are in Figure S1 and Tables S1 and S2, Supporting Information).

These ZW copolymers resemble features of several biological LCDs, including the behavior of upper critical solution temperature (UCST) and the promotion of phase separation at low ionic strength (Figure 1c,d; and Figure S2, Supporting Information). The phase separation is driven by the well-known ion–ion interactions between paired charges, as described in the Collins’ law of matching water affinity where ions of the same size present strong association.^[46] In particular, the similarity in charge densities and hydration between the cationic tertiary ammonium and the anionic sulfate groups confers stronger zwitterionic self-association to the ZB-based polymers compared to the SB-based ones.^[47–49]

Importantly, we found that these attractive interactions mediate the formation of liquid droplets rather than solid aggregates or gels, as revealed by the rapid recovery after photobleaching (Figure 1e) as well as by fusion events between individual droplets in bulk and within microfluidic droplet compartments^[50] (Figure 1f,g). These results reveal a new material state for the ZW polymers, which are already widely used in various architectures, such as protein conjugates, surface coatings, nanoparticles, hydrogels, and liposomes.^[51] Our work here demonstrates that ZW polymers can also form liquid droplets in aqueous solutions.

These ZW droplets are expected to exhibit limited recruitment of client molecules because of the known low protein adsorption properties of zwitterionic polymers when they are used as films or stabilizers of nanoparticles.^[43,45,51] Additionally, we expect that the charges of the monomers are paired and saturated within the polymer droplets due to the attractive intermolecular polymer–polymer forces, and therefore these moieties cannot engage in additional interactions with the client molecules. To verify this hypothesis, we monitored the recruitment of different fluorescent molecules into the ZW coacervates by confocal fluorescence microscopy, measuring the partition coefficient K as the ratio of fluorescence intensities inside and outside the compartments. As expected, droplets formed by the ZW copolymers excluded most tested molecules such as rhodamine B, ATTO647N, bovine serum albumin (BSA), an immunoglobulin (IgG), and dextran macromolecules of different molecular weights (Figure 1h). Moreover, even after incubation with a complex cell lysate containing thousands of different molecules as well as an overexpressed protein, the droplets did not significantly uptake any molecule (Figure 1i).

According to the above results, these ZW droplets are an ideal reference material to establish how the number and type of distinct intermolecular interactions encoded by the scaffold polymers affect the recruitment of different client molecules.

Indeed, the partitioning of specific molecules within the ZW droplets could be regulated by engineering the polymer composition, in particular by progressively adding different functional groups that encode multiple interactions to mimic biological LCD structures (Figure 2a).

Starting from the reference ZW compartments, we introduced a second functional group into the ZW copolymers to encode a second type of intermolecular interaction (Figure 2a). Specifically, we introduced: i) hydroxyl and amide groups (HEMA, a mimic of serine side group and Mam, a mimic of glutamine/asparagine side group) to induce hydrogen bonding; ii) the aromatic benzyl group (BeMA, a mimic of phenylalanine side group) to generate hydrophobic interactions; and iii) the quaternary ammonium group to introduce an unpaired charge encoding electrostatic interactions. All copolymers formed liquid-like droplets as characterized by fusion events (Figure S3, Supporting Information).

For comparison, we characterized the partitioning of different molecules within compartments formed with a lower critical solution temperature (LCST) polymer, namely a poly(ethylene-glycol)-based copolymer (EG, full characterization in Figure S4 and Table S2, Supporting Information) that mainly encodes hydrophobic interactions. We also compared the partitioning within condensates based on a biological LCD protein (LCD of the Ddx4 protein, which is one of the most studied systems of biological condensates^[27]). The hydrophobic compartments based on EG could only recruit the lyophilic rhodamine B (Figure 2b; and Figure S5, Supporting Information). In contrast, condensates formed by the LCD that encodes multiple interactions recruited most of the tested molecules including proteins and dextran, albeit to a different extent (Figure 2b; and Figure S6, Supporting Information).

The introduction of hydrogen bonding (ZWH1-3, full characterization in Tables S1 and S2 and Figure S7, Supporting Information) and aromatic benzyl groups (ZWBe, full characterization in Tables S1 and S2 and Figure S8, Supporting Information) into ZW droplets increased the uptake of small molecules but not of BSA (Figure 2b; and Figure S9, Supporting Information). Introducing the unpaired charge in the ZW polymers (ZW+, full characterization in Table S1 and Figure S10, Supporting Information) promoted the recruitment of BSA but not of rhodamine B (Figure 2b). Adding the unpaired charge in the ZWH copolymers induced an electrostatic interaction in addition to hydrogen bonding. Therefore, this polymer (ZWH+, full characterization in Table S1 and Figure S11, Supporting Information) encodes three different types of interactions and is a better mimic of biological LCDs. Indeed, the corresponding droplets could uptake both rhodamine B and BSA (Figure 2b), confirming that multiple interactions are crucial for modulating the recruitment of molecules with different properties.

We note that the recruitment of the same molecule into different compartments is only partially correlated with the apparent polarity of the coacervates, which was estimated using an assay based on the solvatochromic Prodan dye (Figure 2c; and Figure S12, Supporting Information). The partitioning of rhodamine B is higher in the hydrophobic EG-based compartments, which are characterized by lower polarity. However, the uptake of rhodamine B in ZW and ZWH coacervates was drastically different even though these coacervates had similar

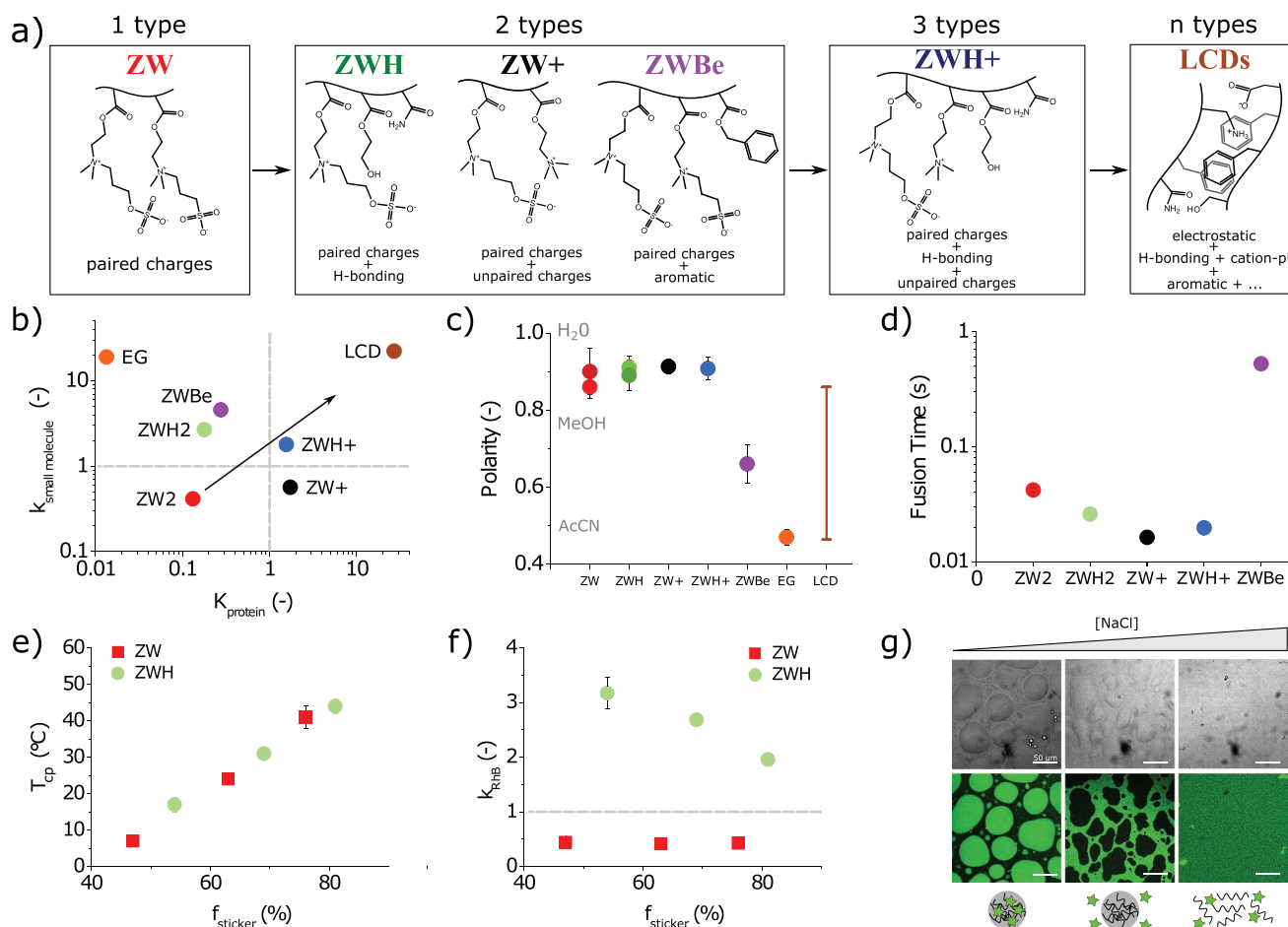


Figure 2. Programming the recruitment and stimulus-responsiveness of droplets by changing the polymer composition. a) Structure of the synthesized polymers encoding a progressively increasing number of interaction types. From the reference ZW, we gradually enhanced the architectural complexity toward mimicking biological LCDs. b) Partition coefficient of rhodamine B and BSA in coacervates of different copolymers. c) Measured relative apparent polarity (with respect to water) of compartments made of different copolymers. For LCDs, the intervals were estimated from published data.^[25,27] d) Fusion time of droplets composed of different copolymers. The error bars are smaller than symbols. e, f) Modulation of the cloud point temperature (e) and the partition coefficient of rhodamine B (f) by increasing the fraction of sticker ZB monomers (f_{ZB}) in ZW and ZWH copolymers. g) Independent control of droplet dissolution and uptake of client molecules allowed the storage droplets to release molecules on demand by changing the environment. Bright-field (top) and fluorescence (bottom) confocal microscopy images for solutions containing 0.25 mg mL^{-1} of ZW+, $1 \times 10^{-6} \text{ M}$ of FITC-BSA, and $135, 430, \text{ or } 500 \times 10^{-3} \text{ M}$ of NaCl (from left to right). This shows that the recruitment of FITC-BSA into ZW+ droplets may be modulated by changing the ionic strength. The droplets only dissolved at higher salt concentrations. ZW: zwitterionic copolymer composed only of zwitterionic moieties. ZWH: copolymer that also contains moieties encoding H-bonding. ZWH+: copolymer exhibiting zwitterionic, H-bonding, and positively charged moieties. ZWBe: zwitterionic polymer that contains both zwitterionic and benzyl (aromatic) moieties.

apparent polarity. These results provide preliminary guidelines for controlling the different mesoscopic properties of polymer droplets by changing the scaffold polymers. The properties include the partitioning of client molecules (Figure 2b), apparent polarity (Figure 2c), and fusion times, which are correlated to the inverse capillary velocity given by the ratio of viscosity to surface tension (η/γ) (Figure 2d).

Moreover, by changing the amount and type of interactions introduced in the copolymer, we can independently modulate different emerging properties of the coacervates. To illustrate this concept, we synthesized ZW and ZWH copolymers with different ratios of the “sticker” ZB monomer that is mainly responsible for the attractive interactions driving phase separation. As expected, the amount of stickers in the ZW copolymer affected the propensity for phase separation, which was estimated by measuring the cloud point temperature via light

scattering (Figure 2e). By changing the type of spacer introduced in the copolymer, we could independently control the partition coefficient of rhodamine B inside the compartments. While the recruitment for all ZW copolymers was low and independent of the ZB molar fraction, the partition coefficient was higher for compartments of ZWH copolymers that encode two types of interactions, to an extent that was proportional to the amount of spacers (Figure 2f).

Overall, these results show that a “sticker and spacer” architecture with at least two monomers encoding two different types of interactions is crucial for controlling multiple properties of the compartments. Here, we could independently regulate the cloud point temperature (Figure 2e) and the recruitment of molecules into the compartments (Figure 2f). A single type of interaction may be sufficient to induce the formation of compartments with different stimulus-responsiveness and

material properties, however it does not allow good control over multiple properties (Figures 1 and 2).

This ability to independently control stimulus-responsiveness and partitioning suggests attractive opportunities for developing biomolecular sorters with programmable partitioning, in which the same stimulus could control the uptake and release of molecules as well as the recovery of the dispersed phase. For instance, copolymers containing unpaired charged groups allow the isolation of biomolecules based on their charge. By modulating the salt concentration at suitable intervals, the uptake and release of the client molecule could be tuned without dissolving the dispersed phase (Figure 2g).

In addition to stimulus-responsiveness (Figures 1 and 2e), viscosity (Figure 1), and recruitment of client molecules (Figure 2b), the composition of the scaffold polymer also determines the surface tension of the compartments, which is associated with the interfacial energy and therefore the miscibility between different compartments. After considering individual coacervates, we next induced the spontaneous formation of distinct compartments and subcompartments in mixtures of different polymers. As a first approximation, we estimated the interfacial energy between different polymers from surface tension measurements via the Girifalco and Good rule^[52] (Figure 3a; and Table S3, Supporting Information). We analyzed the miscibility of pairs of compartments formed by ZW, ZWH, ZWBe, and EG polymers via epifluorescence microscopy. For ZW and ZWH, we also considered the three copolymers containing different fractions of ZB. The staining procedure is described in detail in the Experimental Section.

As predicted by the interfacial energy values (Figure 3a), droplets formed by different ZW copolymers were fully miscible (Figure 3b), while ZW and EG were mutually segregated in their respective compartments to form distinct immiscible droplets (Figure 3c). To the best of our knowledge, this is the first reported example of membraneless polymeric compartments that are fully distinct from each other. The mixtures of ZWBe and three different ZW copolymers with intermediate interfacial tensions generated immiscible compartments with partial wetting (Figure 3d–f). Interestingly, the microstructural organization of the two immiscible phases can be controlled by selecting a suitable pair of copolymers.

We combined the ability to generate droplets with simultaneous control over the structural organization and the uptake of client molecules to replicate cellular organization and create a network of membraneless compartments capable of segregating molecules in space without physical barriers. We generated immiscible droplets composed of ZW+ and ZW2 in both a bulk assay and microfluidic water-in-oil compartments to analyze one single structure (Figure 4). As expected from the partition coefficients measured in individual droplets (Figure 2b), BSA was selectively recruited into the ZW+ compartments. On the other hand, in a generated mixture of immiscible droplets composed of ZWBe and ZW2, the small molecular dye ATTO647N was selectively recruited into the more lipophilic ZWBe droplets, which is consistent with the partition coefficients reported in Figure 2b.

After showing the potential of our polymeric droplets as a model for biological compartmentalization, we tried

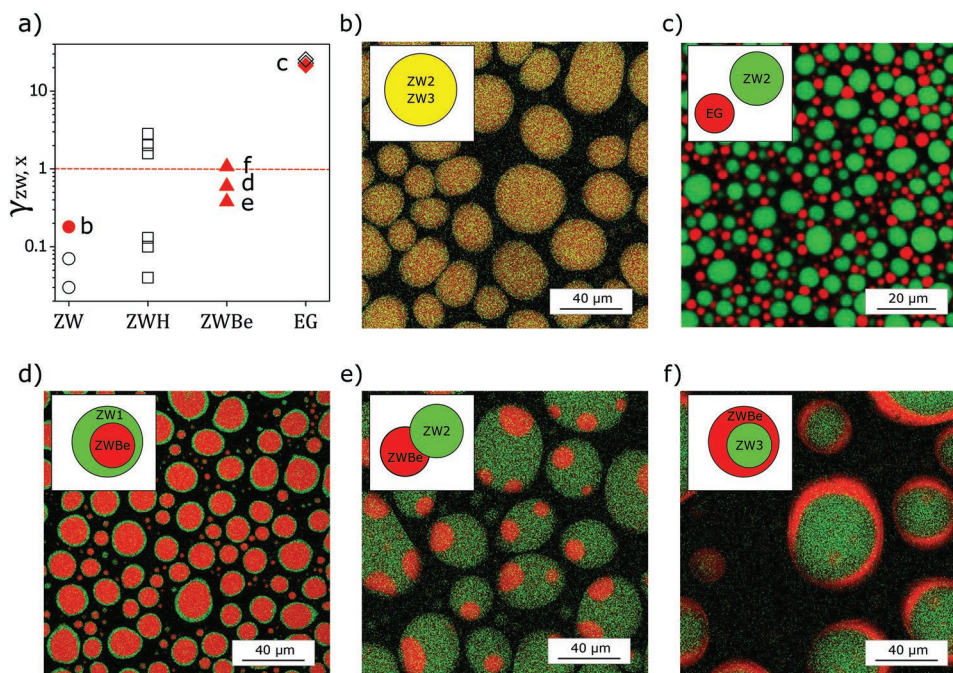


Figure 3. Programming the miscibility of different compartments by changing the polymer composition. a) Estimated interfacial tension between droplets composed of ZW and different copolymers based on the Good–Girifalco rule (Table S3, Supporting Information). For ZW and ZWH, three copolymers containing different fractions of ZB were considered. Each point represents a pair of different copolymers. Labels (b)–(f) indicate the pairs shown in the next panels. b–f) Miscibility between droplets with different compositions can be controlled by selecting a pair of copolymers with suitable interfacial tension. Confocal microscopy images showing the fully miscible ZW2/ZW3 (b), the distinct immiscible compartments of ZW2/EG (c), and immiscible compartments with partial wetting in ZW1/ZWBe (d), ZW2/ZWBe (e), and ZW3/ZWBe (f). For the corresponding interfacial tension see (a).

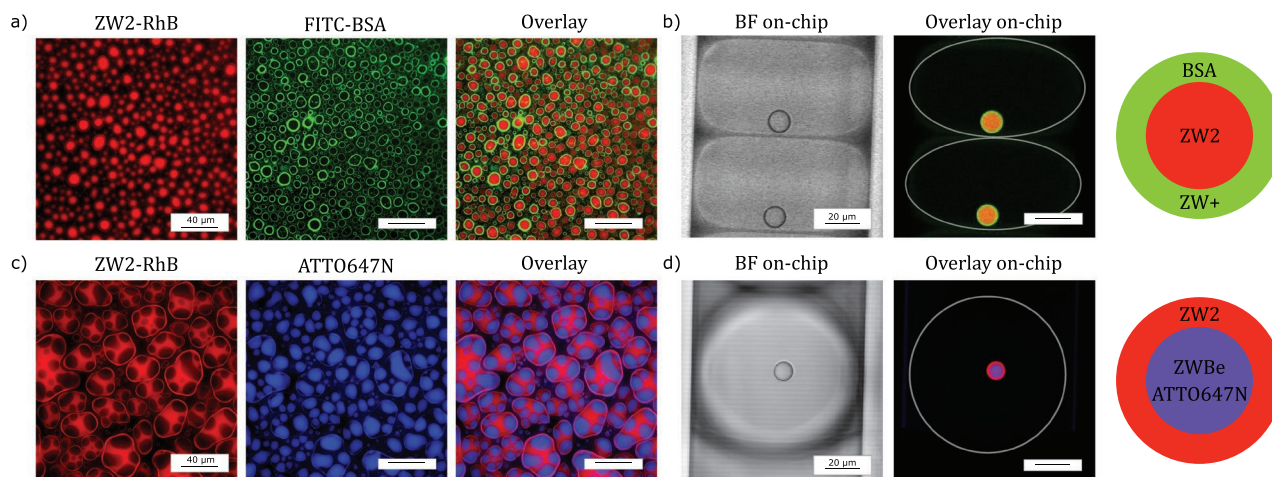


Figure 4. Segregation of molecules between immiscible coexisting membraneless compartments. a,b) Microscopy images of a mixture of immiscible droplets composed of ZW+ and ZW2 conjugated with rhodamine B. The introduced FITC-BSA was selectively recruited into the ZW+ compartments. Bright-field and confocal microscopy images of droplets in the bulk (a) and in microfluidic water-in-oil emulsion compartments (b). c,d) Mixture of immiscible droplets composed of ZWBe and ZW2 conjugated with rhodamine B. The ATTO647N dye was selectively recruited into the more lipophilic ZWBe droplets. Bright-field and confocal microscopy images of droplets in the bulk (c) and in microfluidic droplet compartments (d).

to demonstrate their practical application in bioseparation and diagnostics. Desired molecules over a broad size range can be selectively recruited into the compartments by conjugating the copolymer with a suitable binding partner. The phase-separated droplets may be easily separated from the solution to allow recovery of the target molecules. Importantly, owing to the super-hydrophilicity and lack of protein adsorption on the coacervates, the ZW droplets preferentially excluded most molecules (Figure 1), thereby enabling recovery of the target molecule with high purity even from complex mixtures. We demonstrated this concept by generating ZW copolymers conjugated with biotin, protein A, and streptavidin. Droplets based on these polymers were capable of recruiting streptavidin, an immunoglobulin, and biotin-functionalized vesicles, respectively (Figure 5a). In contrast, the uptake of the molecules into nonfunctionalized ZW-based compartments was negligible ($K = 0.08\text{--}0.36$, Figure 5a). In some cases, the conjugated and non-conjugated polymers formed two immiscible phases, with a shell of conjugated polymers surrounding a core of pure ZW molecules.

Next, we applied the droplets based on ZW conjugated with protein A to isolate IgG molecules from a mixture of multiple proteins and from a cell lysate (Figure 5b). After capturing the IgG molecules, the polymer-rich droplets were separated from the surrounding solution containing the impurities, and the product was recovered after dissolving the droplets at a high ionic strength. Size exclusion chromatography confirmed the selective capture of IgG molecules with a purity of 99.9%. Such capture was not observed in the control ZW droplets lacking protein A (Figure 5b).

This approach has several potential applications ranging from large-scale preparative bioseparation to small-scale diagnostic assays. In the latter case, detection of the target analyte is facilitated by a local increase of its concentration inside the droplets. As proof of concept, we detected streptavidin in fetal bovine serum (FBS) using a ZW-biotin polymer, as shown in Figure 5a. The assay was implemented on a droplet microfluidic platform, in which the solution was compartmentalized in a water-in-oil

emulsion (Figure 5c). Inside each water-in-oil compartment, streptavidin was recruited into the functionalized polymer droplets. The volume of the polymer-rich phase was ≈ 1000 times smaller than that of the external water-in-oil compartment. Thus, assuming that most of the streptavidin molecules were recruited inside the droplet, this method concentrated the protein locally by ≈ 1000 fold.^[53] The labeled streptavidin was detected at a concentration 1×10^{-9} M, which corresponds to less than 1 attomole and ≈ 20 ppm of the total protein mass present in the complex medium consisting of 100% FBS.

3. Conclusion

We have developed programmable liquid droplets based on synthetic responsive polymers inspired by recent observations of cellular compartmentalization. In contrast to the more traditional complex coacervation, here we exploited simple coacervation driven by disordered macromolecules capable of multiple intermolecular interactions. Starting with the zwitterionic polymers, we progressively increased the complexity of their composition toward a better mimic of biological LCDs. We demonstrated that zwitterionic polymers in aqueous solutions can form polymer-rich liquid droplets that largely exclude most molecules, which is a newly reported physical state for these polymers. Then, we gradually added more types of functional groups to this reference material to induce multiple intermolecular interactions. We have shown that this strategy is crucial for simultaneously controlling multiple mesoscopic properties of the droplets, such as stimulus-responsiveness, uptake of client molecules, fusion time, and miscibility. By exploiting the better programmability of our synthetic droplets, we produced a primitive model of cellular compartmentalization based on multiple membraneless compartments that confine molecules in space without physical barriers. Finally, we demonstrated that these biomolecular sorters can locally segregate and increase the concentration of target

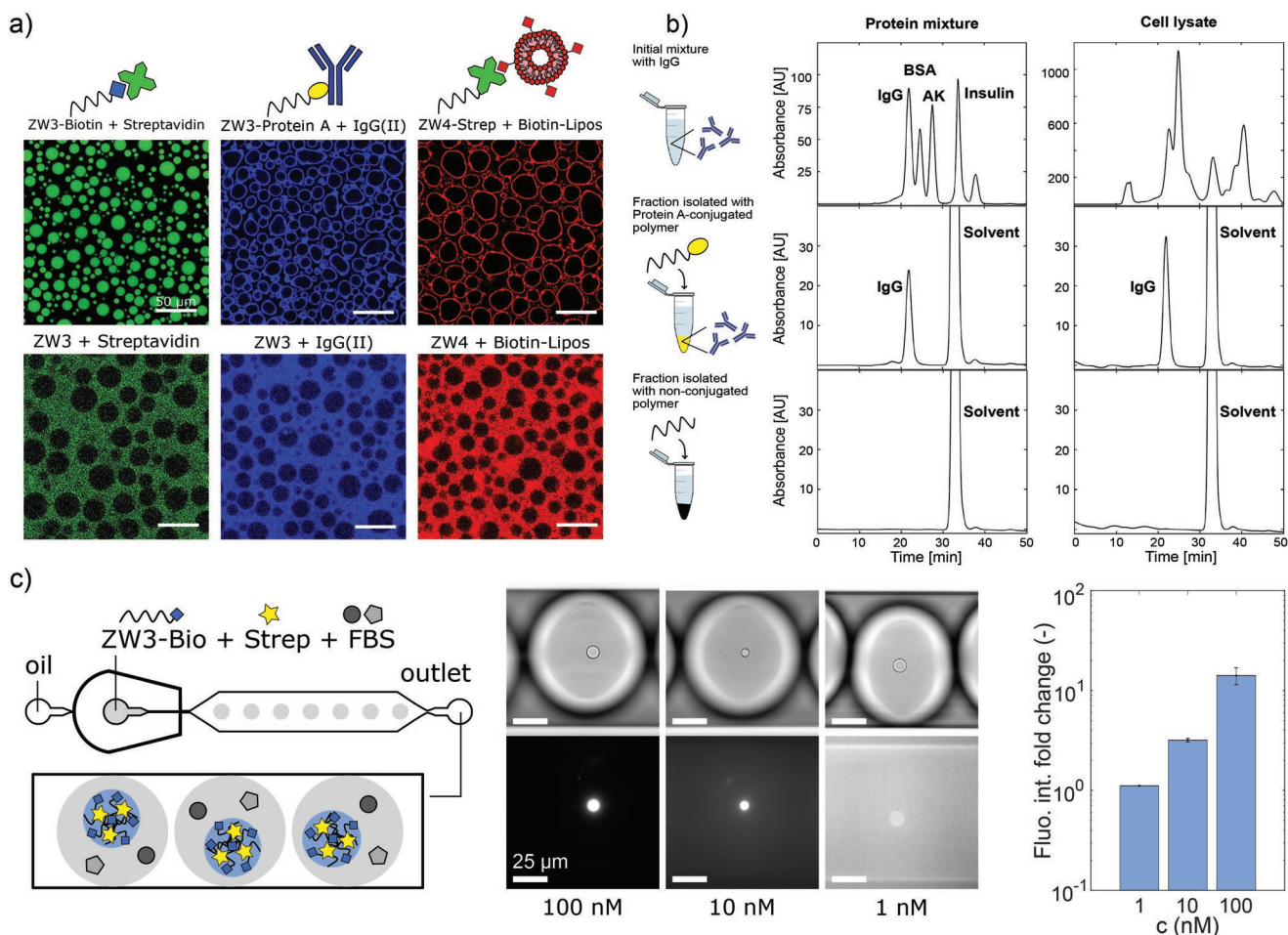


Figure 5. Programmable droplets for biomolecular sorting. a) Confocal microscopy images showing the recruitment of fluorescent streptavidin, IgG, and biotin-labeled liposomes into ZW-based droplets that are respectively functionalized with biotin, protein A, and streptavidin (upper panels). The lower panels show control samples with compartments based on nonfunctionalized ZW polymers, without any significant uptake. b) Isolation of IgG molecules from a mixture of multiple proteins (BSA, adenylate kinase (AK), and insulin) and from a cell lysate by using ZW-droplets conjugated with protein A. Top to bottom: size exclusion chromatograms of the initial mixture, the polymer-rich droplet phase, and the polymer-rich droplet phase of a control polymer without conjugated protein A. The peak at elution time longer than 30 min corresponds to the salt introduced to dissolve the droplets. The full chromatograms are reported in Figure S13 (Supporting Information). c) Detection assay implemented in a droplet-microfluidic platform to quantify nanomolar amounts of labeled streptavidin in fetal bovine serum (FBS). The preferential inclusion of streptavidin within the droplets was quantified as the average fold change in fluorescence intensity inside the polymer droplets relative to the median value of the total water-in-oil compartment. The average values and standard deviations (represented by the error bars) are based on multiple independent droplets (16, 9, and 15 droplets for 1, 10, and 100×10^{-9} M labeled streptavidin, respectively). The difference between the values is statistically significant ($p < 10^{-10}$ using an unpaired *t*-test).

molecules in complex mixtures, with promising application prospects in bioseparation and diagnostics.

Supporting Information

Supporting Information is available from the Wiley Online Library or from the author.

Acknowledgements

The authors gratefully acknowledge Janik Robin Wild, Camilla Stocco, and Nicola Carrara for their assistance with the experiments and ScopeM (ETH Zurich) for their support and assistance in this work. They also thank Dr. Stavros Stavrakis and Prof. Eric Dufresne for discussions and

critical reading of the manuscript. They are grateful to the Swiss National Science Foundation (Grant No. 205321_17905), the Synapsis Foundation for Alzheimer's disease (Zurich), and the Claude & Giuliana Foundation (Zurich) for their financial support. [Correction added on 4 May 2022, after first online publication: CSAL funding statement has been added.]

Open Access Funding provided by Eidgenossische Technische Hochschule Zurich.

Conflict of Interest

The authors declare no conflict of interest.

Data Availability Statement

Research data are not shared.

Keywords

biomolecular condensates, bioseparation, cellular compartmentalization, programmable droplets, responsive polymers, simple coacervates, zwitterionic polymers

Received: June 24, 2021

Revised: October 15, 2021

Published online: November 19, 2021

- [1] B. C. Buddingh, J. C. M. van Hest, *Acc. Chem. Res.* **2017**, *50*, 769.
- [2] B. G. O'Flynn, T. Mittag, *Curr. Opin. Cell Biol.* **2021**, *69*, 70.
- [3] S. F. Banani, H. O. Lee, A. A. Hyman, M. K. Rosen, *Nat. Rev. Mol. Cell Biol.* **2017**, *18*, 285.
- [4] A. S. Lyon, W. B. Peeples, M. K. Rosen, *Nat. Rev. Mol. Cell Biol.* **2021**, *22*, 215.
- [5] Y. Shin, C. P. Brangwynne, *Science* **2017**, *357*, eaaf4382.
- [6] T. Kaur, M. Raju, I. Alshareedah, R. B. Davis, D. A. Potoyan, P. R. Banerjee, *Nat. Commun.* **2021**, *12*, 872.
- [7] M. Feric, N. Vaidya, T. S. Harmon, D. M. Mitrea, L. Zhu, T. M. Richardson, R. W. Kriwacki, R. V. Pappu, C. P. Brangwynne, *Cell* **2016**, *165*, 1686.
- [8] M. Hondele, R. Sachdev, S. Heinrich, J. Wang, P. Vallotton, B. M. A. Fontoura, K. Weis, *Nature* **2019**, *573*, 144.
- [9] M. Kato, T. W. Han, S. Xie, K. Shi, X. Du, L. C. Wu, H. Mirzaei, E. J. Goldsmith, J. Longgood, J. Pei, N. V. Grishin, D. E. Frantz, J. W. Schneider, S. Chen, L. Li, M. R. Sawaya, D. Eisenberg, R. Tycko, S. L. McKnight, *Cell* **2012**, *149*, 753.
- [10] E. W. Martin, T. Mittag, *Biochemistry* **2018**, *57*, 2478.
- [11] E. W. Martin, A. S. Holehouse, I. Peran, M. Farag, J. J. Incicco, A. Bremer, C. R. Grace, A. Soranno, R. V. Pappu, T. Mittag, *Science* **2020**, *367*, 694.
- [12] C. P. Brangwynne, P. Tompa, R. V. Pappu, *Nat. Phys.* **2015**, *11*, 899.
- [13] J. M. Choi, A. S. Holehouse, R. V. Pappu, *Ann. Rev. Biophys.* **2020**, *49*, 107.
- [14] T. M. Franzmann, M. Jahnel, A. Pozniakovskiy, J. Mahamid, A. S. Holehouse, E. Nüske, D. Richter, W. Baumeister, S. W. Grill, R. V. Pappu, A. A. Hyman, S. Alberti, *Science* **2018**, *359*, eaao5654.
- [15] H. G. Bungenberg-de Jong, H. R. Kruyt, *Proc. KNAW* **1929**, *32*, 849.
- [16] P. J. Flory, *J. Chem. Phys.* **1941**, *9*, 660.
- [17] M. Sponchioni, U. Capasso Palmiero, D. Moscatelli, *Mater. Sci. Eng. C* **2019**, *102*, 589.
- [18] C. E. Sing, S. L. Perry, *Soft Matter* **2020**, *16*, 2885.
- [19] J. M. Horn, R. A. Kapelner, A. C. Obermeyer, *Polymers* **2019**, *11*, 578.
- [20] M. Abbas, W. P. Lipiński, J. Wang, E. Spruijt, *Chem. Soc. Rev.* **2021**, *50*, 3690.
- [21] W. C. Blocher, S. L. Perry, *Wiley. Interdiscip. Rev. Nanomed. Nanobio-technol.* **2017**, *9*, 76.
- [22] A. K. Varanko, J. C. Su, A. Chilkoti, *Ann. Rev. Biomed. Eng.* **2020**, *22*, 343.
- [23] M. H. M. E. van Stevendaal, L. Vasiukas, N. A. Yewdall, A. F. Mason, J. C. M. van Hest, *ACS Appl. Mater. Interfaces* **2021**, *13*, 7879.
- [24] M. Dzuricky, B. A. Rogers, A. Shahid, P. S. Cremer, A. Chilkoti, *Nat. Chem.* **2020**, *12*, 814.
- [25] A. M. Küffner, M. Prodan, R. Zuccarini, U. Capasso Palmiero, L. Faltova, P. Arosio, *ChemSystemsChem* **2020**, *2*, 2000001.
- [26] S. Elbaum-Garfinkle, Y. Kim, K. Szczepaniak, C. C. H. Chen, C. R. Eckmann, S. Myong, C. P. Brangwynne, *Proc. Natl. Acad. Sci. USA* **2015**, *112*, 7189.
- [27] T. J. Nott, E. Petsalaki, P. Farber, D. Jervis, E. Fussner, A. Plochowitz, T. D. Craggs, D. P. Bazett-Jones, T. Pawson, J. D. Forman-Kay, A. J. Baldwin, *Mol. Cell* **2015**, *57*, 936.
- [28] B. S. Schuster, R. M. Regy, E. M. Dolan, A. Kanchi Ranganath, N. Jovic, S. D. Khare, Z. Shi, J. Mittal, *J. Phys. Chem. B* **2021**, *125*, 3441.
- [29] C. A. Strulson, R. C. Molden, C. D. Keating, P. C. Bevilacqua, *Nat. Chem.* **2012**, *4*, 941.
- [30] B. S. Schuster, E. H. Reed, R. Parthasarathy, C. N. Jahnke, R. M. Caldwell, J. G. Bermudez, H. Ramage, M. C. Good, D. A. Hammer, *Nat. Commun.* **2018**, *9*, 2985.
- [31] E. Sokolova, E. Spruijt, M. M. K. Hansen, E. Dubuc, J. Groen, V. Chokkalingam, A. Piruska, H. A. Heus, W. T. S. Huck, *Proc. Natl. Acad. Sci. USA* **2013**, *110*, 11692.
- [32] N. Martin, *ChemBioChem* **2019**, *20*, 2553.
- [33] K. Lasker, S. Boeynaems, V. Lam, E. Stainton, M. Jacquemyn, D. Daelemans, E. Villa, A. S. Holehouse, A. D. Gitler, L. Shapiro, *bioRxiv* **2021**, <https://doi.org/10.1101/2021.02.03.429226>.
- [34] G. A. Mountain, C. D. Keating, *Biomacromolecules* **2020**, *21*, 630.
- [35] T. Lu, E. Spruijt, *J. Am. Chem. Soc.* **2020**, *142*, 2905.
- [36] W. C. Blocher McTigue, S. L. Perry, *Small* **2020**, *16*, 1907671.
- [37] N. A. Yewdall, A. A. M. André, T. Lu, E. Spruijt, *Curr. Opin. Colloid Interface Sci.* **2021**, *52*, 101416.
- [38] U. Capasso Palmiero, A. M. Küffner, F. Krumeich, L. Faltova, P. Arosio, *Angew. Chem., Int. Ed.* **2020**, *59*, 8138.
- [39] L. Faltova, A. M. Küffner, M. Hondele, K. Weis, P. Arosio, *ACS Nano* **2018**, *12*, 9991.
- [40] K. M. Ruff, F. Dar, R. V. Pappu, *Proc. Natl. Acad. Sci. USA* **2021**, *118*, 2017184118.
- [41] J. M. Choi, F. Dar, R. V. Pappu, *PLoS Comput. Biol.* **2019**, *15*, e1007028.
- [42] N. M. Nizardo, D. Schanzenbach, E. Schönemann, A. Laschewsky, *Polymers* **2018**, *10*, 325.
- [43] M. Sponchioni, P. R. Bassam, D. Moscatelli, P. Arosio, U. C. Palmiero, *Nanoscale* **2019**, *11*, 16582.
- [44] N. Morimoto, Y. Oishi, M. Yamamoto, *Macromol. Chem. Phys.* **2020**, *221*, 1900429.
- [45] E. Schönemann, A. Laschewsky, E. Wischerhoff, J. Koc, A. Rosenhahn, *Polymers* **2019**, *11*, 1014.
- [46] C. J. Fennell, A. Bizjak, V. Vlachy, K. A. Dill, S. Sarupria, S. Rajamani, S. Garde, *J. Phys. Chem. B* **2009**, *113*, 14837.
- [47] Q. Shao, S. Jiang, *Adv. Mater.* **2015**, *27*, 15.
- [48] Q. Shao, S. Jiang, *J. Phys. Chem. B* **2014**, *118*, 7630.
- [49] Q. Shao, L. Mi, X. Han, T. Bai, S. Liu, Y. Li, S. Jiang, *J. Phys. Chem. B* **2014**, *118*, 6956.
- [50] M. Linsenmeier, M. R. G. Kopp, F. Grigolato, L. Emmanoulidis, D. Liu, D. Zürcher, M. Hondele, K. Weis, U. Capasso Palmiero, P. Arosio, *Angew. Chem., Int. Ed.* **2019**, *58*, 14489.
- [51] A. Erfani, J. Seaberg, C. P. Aichele, J. D. Ramsey, *Biomacromolecules* **2020**, *21*, 2557.
- [52] R. J. Good, L. A. Girifalco, *J. Phys. Chem.* **1960**, *64*, 561.
- [53] M. R. G. Kopp, M. Linsenmeier, B. Hettich, S. Prantl, S. Stavrakis, J. C. Leroux, P. Arosio, *Anal. Chem.* **2020**, *92*, 5803.